Crystal Channelling for Hadron Therapy Accelerators

CERN Summer Student Programme 2022

Ng Hoi Lun*
Department of Physics, The Chinese University of Hong Kong

Advisors: Prof. Kenneth Long and Rebecca Louise Taylor
(Dated: August 12, 2022)

In this study, the effect of crystal channelling in low energy (kinetic energy from 60 to 250 MeV) proton beam which is the energy range required for hadron therapy treatments in a medical accelerator is investigated. This was investigated using a Monte-Carlo simulation programme which combined beam dynamic simulations with particle-matter interactions. The behaviour of the crystal was explored both in isolation, to understand its physical properties, and within the context of a full accelerator, to replace an extraction septum magnet used in the Proton-Ion Medical Machine Study (PIMMS) synchrotron. The study analysed the channelling effect under various beam energies and found that the channelling effect, with many real-life application potential, was difficult to obtain at low energies. Moreover, it was shown and explained that there exists an optimal set of bending angles and crystal lengths for particular beam energy.

I. INTRODUCTION

Crystal channelling is a process that bends charged particles using the cumulative electrostatic forces from the lattice structure of a crystal. It has a great prospect in accelerator-related applications, especially as a replacement for kicker magnets. Compared to a conventional kicker magnet, a crystal channelling device does not need power and is much smaller, making it a perfect candidate. While many studies on crystal channelling have been conducted, most of them are focusing on the application with high-energy beam as used in the Super Proton Synchrotron (450 GeV) and Large Hadron Collider (7 TeV). Yet, crystal channelling is also appealing for low-energy accelerators due to its compact size. In this report, the crystal channelling effect with a low-energy beam and in a medical accelerator will be studied by making use of a simulation programme called Beam Delivery SIMulation (BDSIM) [1].

II. A QUALITATIVE VIEW ON THE THEORY

When a particle enter a well-aligned crystal, it will see a continuous potential set up by the periodic structure of the crystal which is the combination of Moliere potentials from the nearby planes of atoms as shown in Fig. 1 [2]. The potential well traps the particles with low enough energy and thus forces the particle to move along the gaps between the planes. This is called the channelling effect. This reduces angular scattering and energy loss caused by the collisions between the particles and the nuclei [2]. If the crystal is slightly bent, the potential will remain virtually the same and the particles will bend with the crystal but with a lower potential due to the centrifugal force [2]. A higher fraction of escapement is thus expected.

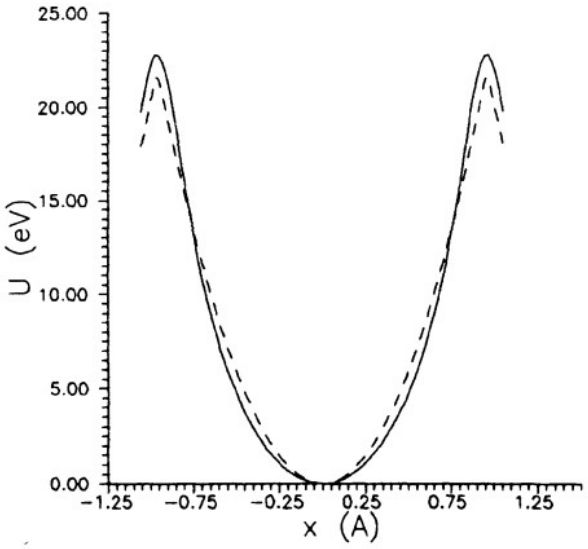

FIG. 1: The interplanar Moliere potential of Si110 crystal that seen by the particles [2]. A harmonic approximation is plotted alongside using a dashed line [2].

Besides, not all particles will be channelled. When the particles interact with the atoms, some of them will receive a kick. When the kick is too strong or with a channelled angle (defined by $\theta = \frac{dx}{dz} = x_p$) larger than some critical value and in the opposite direction, the particle will escape the potential well and become dechannelled [2, 3].

To study the dechannelled effect, the diffusion approach is usually adopted [2]. This model suggests that:

$$\text{Fraction of channelled particle} \sim \exp(-z/L_D) \quad (1)$$

* hoi.lun.ng@cern.ch; boris.ng125@gmail.com

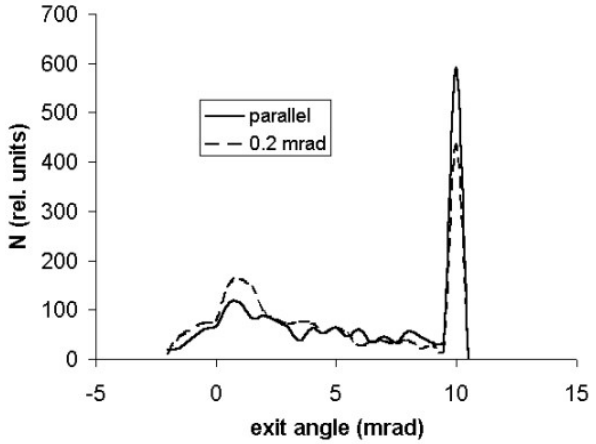

FIG. 2: The simulated angular distribution of 1 GeV protons after hitting a silicon crystal bent 10 mrad [4]. The solid line corresponds to a parallel incident beam while the dotted line refers to a beam with a divergence of 0.2 mrad [4].

$$L_D(pv, R) \sim \frac{E_c(pv/R)}{E_c(0)} \tag{2}$$

where z is the distance travelled in the crystal, L_D is the dechannelling length and E_c is the potential at the critical transverse coordinate for channelled particle that depends on the particle momentum p, velocity v and crystal curvature $1/R$. Generally, L_D decreases with smaller pv and thus smaller beam energy.

Combining the channelling and dechannelling effect, this means that there is a spread of exit angle θ_{out} as indicated by Fig. 2.

III. CRYSTAL IN ISOLATION

A. Methodology

The crystal is modelled and simulated using BDSIM with the codes attached in Appendix A 1. The setup is as followed: 3 identical drift tubes of 1 cm are placed before the crystal. A box-shaped silicon 110 (Si110) crystal with varying length, varying bending angle and fixed cross-section size of 4 cm×4 cm is placed in the middle of a collimator of length 30 mm. Moreover, the crystal is rotated by half the bending angle. Lastly, there is a 3 m drift tube with an aperture radius of 1.5 m.

On the other hand, to have a simple and repeatable proton beam, a square distribution is adopted. The beam has a envelope in x and x_p of 0.4 cm and 5×10^{-4} respectively while having a 0 envelope in y and y_p. The beam energy will be varied to different values to study the channelling effect.

B. Findings and discussion

1. Varying Energy

This section is dedicated to see the limit of channeling as a function of energy for static crystal parameters. In this simulation, a crystal with a bending angle 150 µrad and a length of 2 mm is used. Besides, the beam energy is varied from 400 GeV to 1.078 GeV (KE = 140 MeV) with uneven steps. The exact energies used can be found in Appendix B 1. To have good statistical precision, 10000 particles are used in the simulation.

By plotting $\theta_{out} - \theta_{in}$ against θ_{in} where $\theta = x_p$ as before, it was found that the channeled particle would form a diamond-shaped region. Moreover, it is observed that at high energy, there is a small range of θ_{in} that can lead to channelling with a limited range of $\theta_{out} - \theta_{in}$ values. The opposite was found at low energy, namely that both θ_{in} and $\theta_{out} - \theta_{in}$ both have a large spread. On the other hand, there is a dechannelled region observed in the graphs which have positive $\theta_{out} - \theta_{in}$ values. Like its diamond-shaped counterpart, these regions would grow in size in both θ_{in} and $\theta_{out} - \theta_{in}$ direction at higher energy and shrink at lower energy. At low to medium energies, the channelled particles will even be channelled to other directions but still with a smaller θ than the dechannelled particles. All graphs can be found in the Appendix C 1.

It is particularly interesting to study the graph at the low energy of 1.078 GeV since it is roughly the energy that the PIMMS machine supply for medical use. At such low energy, the graph becomes quite unlike its high energy counterpart. Note that there is only one distinct region on the graph. This diamond-shaped section should be due to the channelling effect. However, the spread is so large that it is difficult to isolate and extract the particles bending correctly (i.e. with negative $\theta_{out} - \theta_{in}$).

From the above data, note that the channelled particles form an almost perfect diamond which agrees with Laurie's result [5]. However, bare in mind that this perfect shape stems from the artifact of simulation and thus is unphysical. To get back a more realistic result, a Gaussian smearing should be applied [5]. Moreover, it is pretty clear that a crystal with properties of 150 150 µrad and 2 mm does not demonstrate channelling at low energies used in hadron therapy treatment. At such energies, although channelling is still observed, the quality of the exiting beam is so poor that a noticeable amount of the channelled particles are funnelled into the wrong direction. On the contrary, for higher energy protons, even as low as 2 GeV, a distinctive channelling and a dechannelling region can be observed. This means that crystal channelling is applicable for medium to high-energy proton beams. However, at high energy for this particular crystal design, due to the large proportion of dechannelled particles, it may be more efficient to use the dechannelled particles instead.

The reason for the strange channelling behaviour at low energy can be explained by well-known physics.

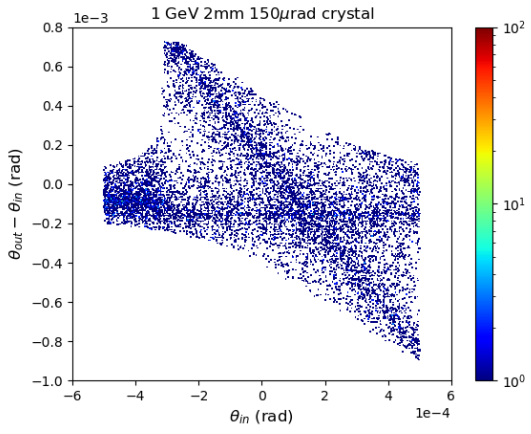

(a)

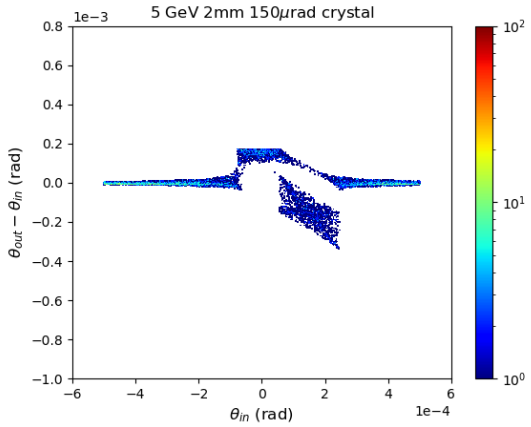

(b)

FIG. 3: (a) and (b) are the $\theta_{out} - \theta_{in}$ against θ_{in} plots of 1.078 GeV (KE = 140 MeV) and 5 GeV protons beam respectively. (a) is titled "1 GeV" just for formatting reasons. Note that (a) and (b) looks rather different. (a) is much messier and only have the diamond region.

First, the spreading in θ_{in} can be understood with volume capture. Just like how channelled particles can be dechannelled by receiving random kicks through interaction with the atoms, some originally dechannelled particles can receive kicks to become channelled. This process is called volume capture and its probability w_S increase with lower momentum and thus lower beam energy [2]:

$$w_S = \text{const}\frac{R}{(pv)^{3/2}} \tag{3}$$

This means that volume channelling is more prominent at lower energies. Therefore, at lower and lower energies, more and more originally dechannelled particles near the channelling θ_{in} can be kicked into a channelling state through volume capture. This explains the spreading of the diamond on the x-axis.

Second, the spreading in $\theta_{out} - \theta_{in}$ can be studied using

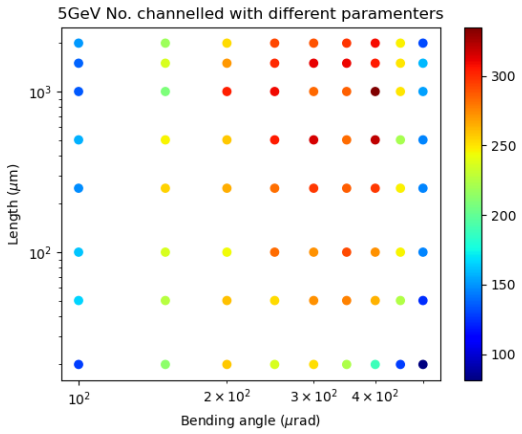

FIG. 4: This plot shows the number of channelled particles with different bending angles and lengths of crystal. The number of particles is shown by the colour.

the diffusion approach. In Section II, the concept of the diffusion approach is already established. The main point is that by Eq. 1 and 2, the channelled fraction is given by $\exp(-z/L_D)$ and L_D decreases with decreasing beam energy. So, at low energies, fewer particles are able to be channelled at the same distance in the crystal. As a result, some particles become dechannelled, leading to a spread in θ_{out} and thus $\theta_{out} - \theta_{in}$.

2. *Varying crystal length and bending angle*

After seeing how varying the energy will affect the channelling pattern and channelling effect, we tried to see how crystal length and bending angle affect channelling. In this section, a 5 GeV energy beam with 2000 particles is used. The crystal length is varied from 2 mm to 20 µm with uneven steps. Similarly, a bending angle from 500 µrad to 100 µrad is tested with uneven steps. The exact angle and length used can be found in Appendix B 2. The crystal is put into a collimator in a similar way as Section III B 1. The goodness of channelling is analyzed by counting the number of particles with $\theta_{out} - \theta_{in}$ lower than a threshold value of -1×10^{-4}.

By plotting the number of channelled particles with various bending angles and crystal length in Fig. 4, their effect on channelling can be studied. It was found that a small bending angle or crystal length would decrease the number of channelled particles. Similarly, a large bending angle or crystal length would also lower the channelled number. This means that there is a optimal bending angle and crystal length.

This result agrees well with our intuition. First, for same length, a low bending angle would result in relatively few channelled particles. This is because the bending is smaller and thus when some particles get dechannelled mid way, many will not be bent to a θ smaller

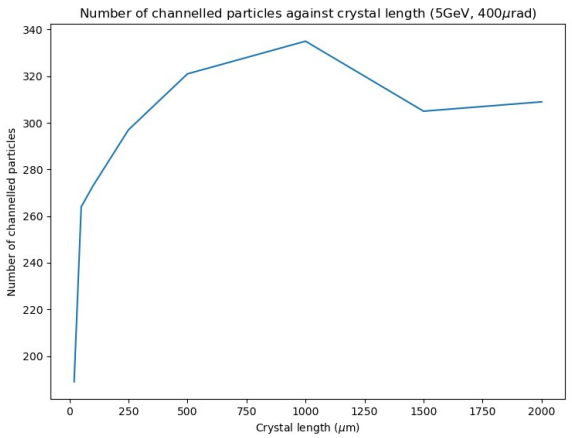

FIG. 5: This graph plots the number of channelled particles against crystal length with beam energy and crystal bending angle of 5 GeV and 400 µrad. It is a slice of Fig. 4.

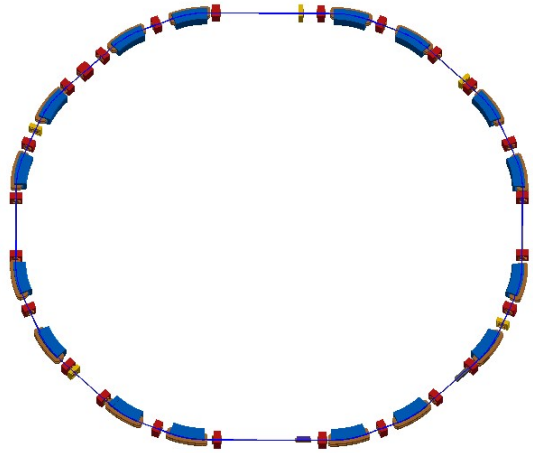

FIG. 6: This is the PIMMS machine lattice visualized in BDSIM. The crystal and collimator are located roughly at the 4 o'clock position in the figure. It is represented by a grey rectangle box.

than the threshold value. Therefore, the channelling effect would improve with a larger bending angle. However, there is a upper limit since a larger bending angle would lower the interplanar potential more by the centrifugal force.

On the other hand, a short crystal would not channel many particles since the particles do not stay in the crystal for enough time for bending. Such crystal would mostly scatter the particles instead of channelling them. Yet, a long crystal would not necessarily increase the channelled number. Remember Eq. 1, the channelled fraction follows $\exp(-z/L_D)$, so a longer crystal would decrease the number of channelled particles. This can be clearly seen in Fig. 5.

From the simulation, the optimal set of parameters should be around 400 µrad and 1 mm.

IV. CRYSTAL IN PIMMS

A. Methodology

A stable beam PIMMS machine lattice [6] written in Mad-X format is provided by Rebecca Taylor. The lattice is then converted to a BDSIM readable gmad format using tools from BDSIM. Moreover, a Si110 crystal of length 2 mm and bending angle 150 µrad is used. It is put in a collimator like that in Section III B 1 but with a length of 80 cm. To see the effect of the crystal, another simulation with a 80 cm drift tube replacing the crystal and collimator is run and compared. The beam kinetic energy is set to 1.2 GeV which is the maximum the PIMMS machine can deliver. Due to limited time, only 50 turns and 2000 particles are simulated. The BDSIM code for the beam line is attached in the Appendix A 2.

1. *Findings and discussion*

First, phase diagrams of the crystal-containing and the drift tube-containing lattice at different turn number are plotted to study the effect of the crystal. The phase data is collected right after the crystal collimator or the drift tube. Note that the phase diagrams are attached in Appendix C 2.

At first glance, the phase diagrams between the two lattices are pretty similar. The only difference is that the phase diagrams for crystal has a slightly larger spread in x. This effect can be more easily spotted with higher turn number. This is due to the channelling and dechannelling effect which give a boost of $\theta = x_p$ and in turn give a larger distribution in x and x_p. However, the original x_p is in the order of 10^{-2} which masks the 10^{-4} spreading by channelling or dechannelling effect. Therefore, only x which has a order of 10^{-3} reflects the crystal effect.

On the other hand, a plot of the number of particle after passing through the crystal or drift tube against the turn number is generated. The PIMMS machine with the crystal shows a more significant drop in particle number. This may show that crystal effects is applicable for beam extraction at future generations of medical accelerator which makes use of GeV scale energy. It is also important to keep in mind that the large beam loss in the drift tube scenario demonstrates that the optics in the BDSIM model of the PIMMS machine have not been fully optimized.

However, due to time restriction, the number of particles and turn numbers are restricted to a relatively small number. To have a concrete study on the feasibility of using crystal for beam extraction, one should increase these two parameters. Moreover, the beam interaction with the lattice depends heavily on the initial condition

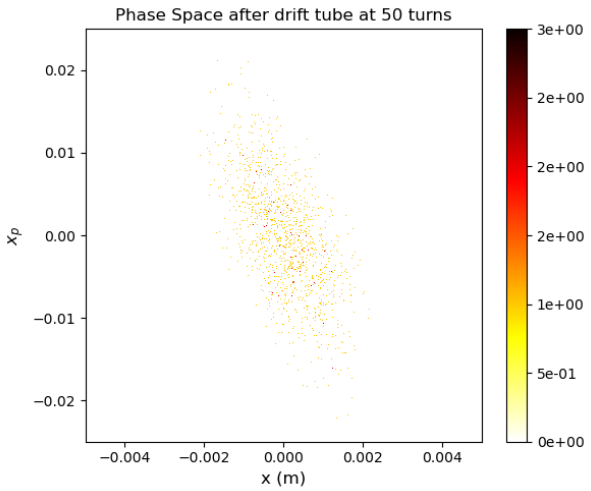

(a)

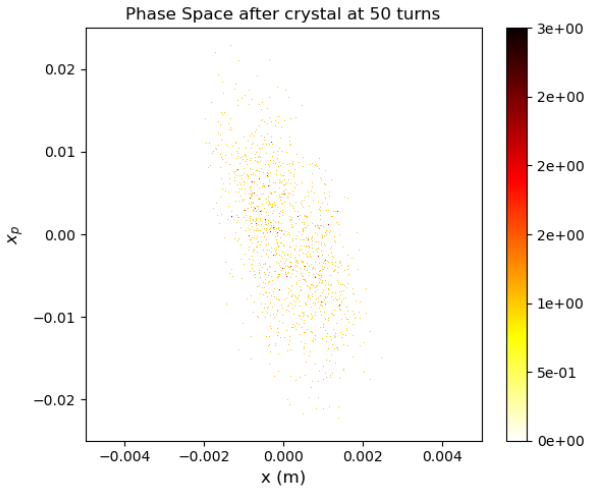

(b)

FIG. 7: (a) and (b) are the phase diagram generated using the drift tube and the crystal lattice respectively at 50 turns. These two graphs are only slightly different, namely that (a) has a smaller spread in x.

which is randomized. One should run the programme more than one time to obtain a more representative result and plot error bars.

V. CONCLUSION

In this work, we show that for the explored parameter space for crystal design, channelling is not applicable for low energy proton beam that is commonly used in current medical accelerators. Besides, the channelling effect of medium to high energy proton beam is also investigated. It was found that the channelling region would have a increasing spread in θ_{in} and $\theta_{out} - \theta_{in}$. This phenomenon is explained using volume capture and diffusion approach. Moreover, the effect of bending angle and crystal length on channelling is studied. It is shown and explained that an optimal set of parameter should exist. In the case of 5 GeV proton beam, the values should be around 400 µrad and 1 mm. Finally, the feasibility of using crystal channelling for beam extraction is studied using the PIMMS machine in high energy setting. It was discovered that crystal can lead to substantially more particle loss which may indicate that the possibility of a crystal channelling-based beam extraction mechanism in future higher energy medical accelerators. However, it must be noted that more simulation must be done before reaching a credible conclusion.

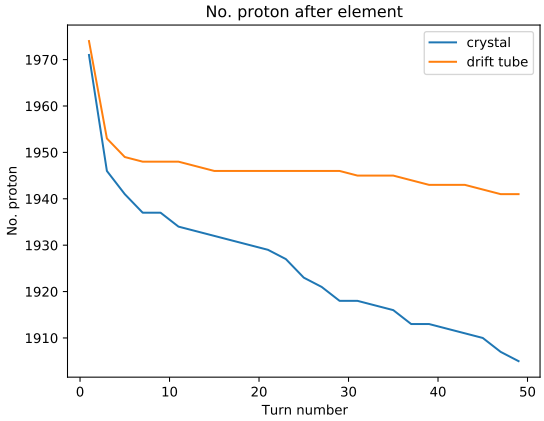

FIG. 8: This graph shows the number of particles after passing through the crystal or drift tube against the turn number. It is obvious that the lattice with crystal shows a more significant drop in particle number.

ACKNOWLEDGMENTS

I would like to thank Prof. Kenneth Long and Rebecca Taylor for their help and guidance in the project. Moreover, I wish to show my gratitude to Dr. William Shields and Dr. Laurence Nevay for their support in BDSIM and crystal channelling. Without these people, I could not complete this project.

[1] L. Nevay, S. Boogert, J. Snuverink, A. Abramov, L. Deacon, H. Garcia-Morales, H. Lefebvre, S. Gibson, R. Kweehinzmann, W. Shields, and S. Walker, Bdsim: An accelerator tracking code with particle–matter interactions,

Computer Physics Communications **252**, 107200 (2020).
[2] V. M. Biryukov, Y. A. Chesnokov, and V. I. Kotov, *Crystal channeling and its application at high-energy accelerators* (Springer Science & Business Media, 2013).
[3] V. Biryukov, Volume reflection efficiency for negative particles in bent crystals, Physics Letters B **765**, 276 (2017).
[4] S. Bellucci and V. Biryukov, Possibility of crystal extraction and collimation in the sub-gev range, Physical Review Special Topics-Accelerators and Beams **10**, 013501 (2007).
[5] L. Nevay, Status of crystal simulations with the geant4 routine (2020).
[6] L. Badano, M. Benedikt, P. J. Bryant, M. Crescenti, P. Holy, A. T. Maier, M. Pullia, S. Rossi, and P. Knaus (CERN-TERA Foundation-MedAustron Oncology-2000 Collaboration), *Proton-Ion Medical Machine Study (PIMMS), 1* (1999).

Appendix A: Simulation codes

1. Crystal in isolation

a. *Varying energy*

```
VAR1 = 150*urad;

Si_crystal: crystal, material = "G4_Si",
        data = "/afs/cern.ch/user/h/hng/bdsim_crystal/data/Si220pl",
        shape = "box",
        lengthY = 4*cm,
        lengthX = 4*cm,
        lengthZ = 2*mm,
        sizeA = 5.43*ang,
        sizeB = 5.43*ang,
        sizeC = 5.43*ang,
        alpha = 1,
        beta = 1,
        gamma = 1,
        spaceGroup = 227,
        bendingAngleYAxis = VAR1,
        bendingAngleZAxis=0;

cry_col1: crystalcol, l=30*mm, apertureType="rectangular", aper1=10*cm, aper2=10*cm, crystalRight="
    Si_crystal", xsize=-2*cm, crystalAngleYAxisRight=-0.5*VAR1;

d1: drift, l = 1*cm, aper1=10*cm;
d2: drift, l = 3*m, aper1=1.5*m;
l1: line = (d1, d1, d1, cry_col1, d2);
use, l1;
sample, all;

beam, particle="proton",
    energy = $VARR*GeV,
    distrType = "square",
    envelopeX = 4*cm/10,
    envelopeXp = 1e-3/2;

option, physicsList="channelling", stopSecondaries=1;
```

Listing 1: This is the code for simulations that vary the beam energy. Note that the energy is specified by $VARR which will be modified with a simple python script.

b. *Varying crystal length and bending angle*

```
VAR1 = $VARR1*urad;
VAR2 = $VARR2*um;

Si_crystal: crystal, material = "G4_Si",
        data = "/afs/cern.ch/user/h/hng/bdsim_crystal/data/Si220pl",
        shape = "box",
        lengthY = 4*cm,
        lengthX = 4*cm,
```

```
9           lengthZ = VAR2,
10          sizeA = 5.43*ang,
11          sizeB = 5.43*ang,
12          sizeC = 5.43*ang,
13          alpha = 1,
14          beta = 1,
15          gamma = 1,
16          spaceGroup = 227,
17          bendingAngleYAxis = VAR1,
18          bendingAngleZAxis=0;
19
20  cry_col1: crystalcol, l=30*mm, apertureType="rectangular", aper1=10*cm, aper2=10*cm, crystalRight="
        Si_crystal", xsize=-2*cm, crystalAngleYAxisRight=-0.5*VAR1;
21
22  d1: drift, l = 1*cm, aper1=10*cm;
23  d2: drift, l = 3*m, aper1=1.5*m;
24  l1: line = (d1, d1, d1, cry_col1, d2);
25  use, l1;
26  sample, all;
27
28  beam, particle="proton",
29      energy = 5*GeV,
30      distrType = "square",
31      envelopeX = 4*cm/10,
32      envelopeXp = 1e-3/2;
33
34  option, physicsList="channelling", stopSecondaries=1;
```

Listing 2: This is the code for simulations that vary the crystal bending angle and length. Note that the angle and length are specified by $VARR1 and $VARR2 which will be modified with a simple python script.

2. CRYSTAL IN PIMMS

```
1   l0: line = (DRIFT_0, PIMMS_CAVITY, DRIFT_1, DRIFT_2, QF1, DRIFT_3, MB,
2       DRIFT_4, QD, DRIFT_5, MB, DRIFT_6, QF1, DRIFT_7, DRIFT_8, XCD1,
3       DRIFT_9, QF2, DRIFT_10, MB, DRIFT_11, QD, DRIFT_12, MB, DRIFT_13, QF2,
4       DRIFT_14, DRIFT_15, QF2, DRIFT_16, MB, DRIFT_17, QD, DRIFT_18, XCF1,
5       DRIFT_19, MB, DRIFT_20, QF2, DRIFT_21, QA, DRIFT_22, QF1, DRIFT_23,
6       MB, DRIFT_24, QD, DRIFT_25, MB, DRIFT_26, QF1, DRIFT_27, XRR,
7       DRIFT_28, QF1, DRIFT_29, MB, DRIFT_30, QD, DRIFT_31, MB, DRIFT_32,
8       QF1, DRIFT_33, XCD2, DRIFT_34, QF2, DRIFT_35, MB, DRIFT_36, QD,
9       DRIFT_37, MB, DRIFT_38, QF2, DRIFT_39, QF2, DRIFT_40, MB, DRIFT_41,
10      QD, DRIFT_42, XCF2, DRIFT_43, MB, DRIFT_44, QF2, DRIFT_45);
11
12  l0_cont: line = (DRIFT_46, QF1, DRIFT_47, MB, DRIFT_48, QD, DRIFT_49, MB, DRIFT_50,
13      QF1, DRIFT_51);
14
15  DRIFT_52_short: drift, l=1.33775-0.2*um; !-0.2 um to satisfy the req of BDSIM for circular machine
16
17  l1: line = (MS, DRIFT_52_short);
18
19  VAR1 = 150*urad;
20  VAR2 = 2;
21
22  Si_crystal: crystal, material = "G4_Si",
23          data = "/afs/cern.ch/user/h/hng/bdsim_crystal/data/Si220pl",
24          shape = "box",
25          lengthY = 4*cm,
26          lengthX = 4*cm,
27          lengthZ = 2*mm,
28          sizeA = 5.43*ang,
29          sizeB = 5.43*ang,
30          sizeC = 5.43*ang,
31          alpha = 1,
32          beta = 1,
33          gamma = 1,
34          spaceGroup = 227,
```

```
35          bendingAngleYAxis = VAR1,
36          bendingAngleZAxis=0;
37
38  Drift_temp: drift, l=0.8, apertureType="rectangular", aper1=10*cm, aper2=10*cm;
39
40  cry_col: crystalcol, l=0.8, apertureType="rectangular", aper1=10*cm, aper2=10*cm, crystalRight="
        Si_crystal", xsize=-2*cm, crystalAngleYAxisRight=-0.5*VAR1;
41
42  lattice: line = (l0, cry_col, l0_cont, l1); !Drift_temp
43  use, period=lattice;
44  option, circular=1, nturns=51, physicsList=``channelling'';
```

Listing 3: This is the code for simulations of PIMMS lattice with the crystal and collimator. Please change line 42 from "cry_col" to "Drift_temp" to replace with drift tube.

Appendix B: Parameters in simulations

1. Varying energy

Beam energies (GeV) used in simulation:

1.078	2	3	5	7
10	25	50	75	100
200	400			

2. Varying crystal length and bending angle

Bending angles (μrad) used in simulation:

100	150	200	250	300
350	400	450	500	

Crystal length (μm) used in simulation:

20	50	100	250	500
1000	1500	2000		

Appendix C: Graphs in simulation

1. Varying energy

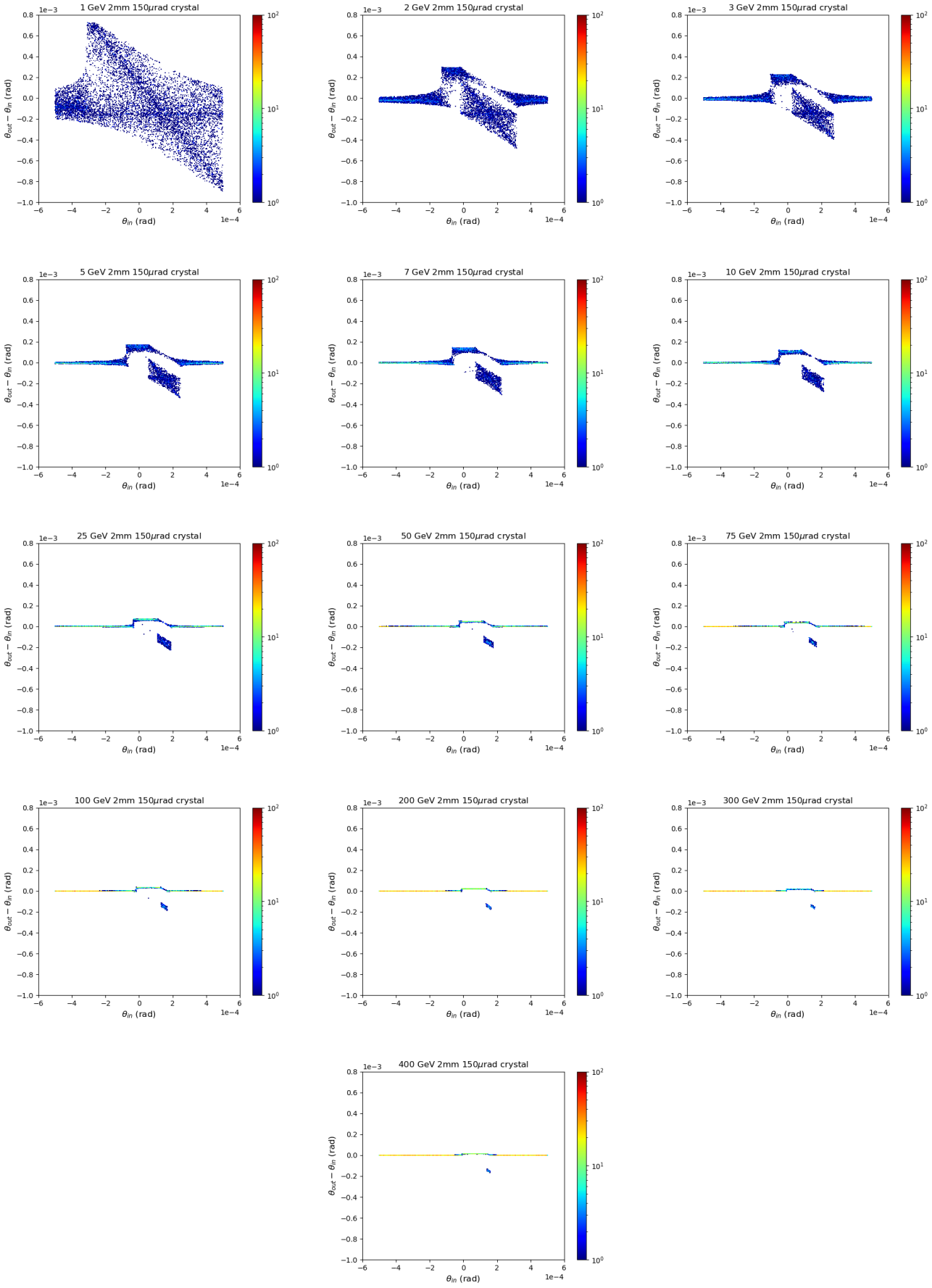

FIG. 9: The $\theta_{out} - \theta_{in}$ against θ_{in} graphs at different energies. The corresponding beam energy can be read from the title but note that 1 GeV refers to 1.078 GeV. An animation of these can be found here.

2. Crystal in PIMMS

a. Lattice with drift tube

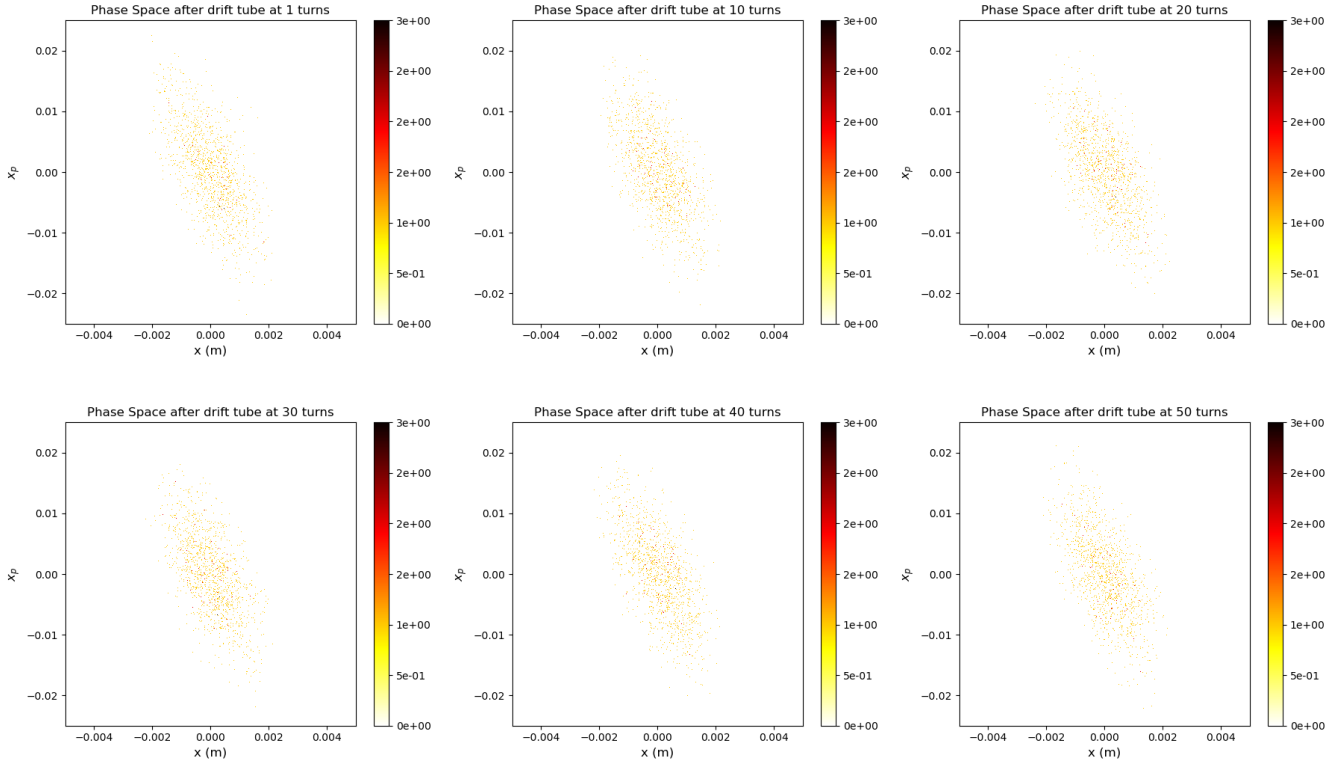

FIG. 10: The phase diagram after the drift tube at nth turns. The corresponding turn number can be read from the title.

b. Lattice with crystal

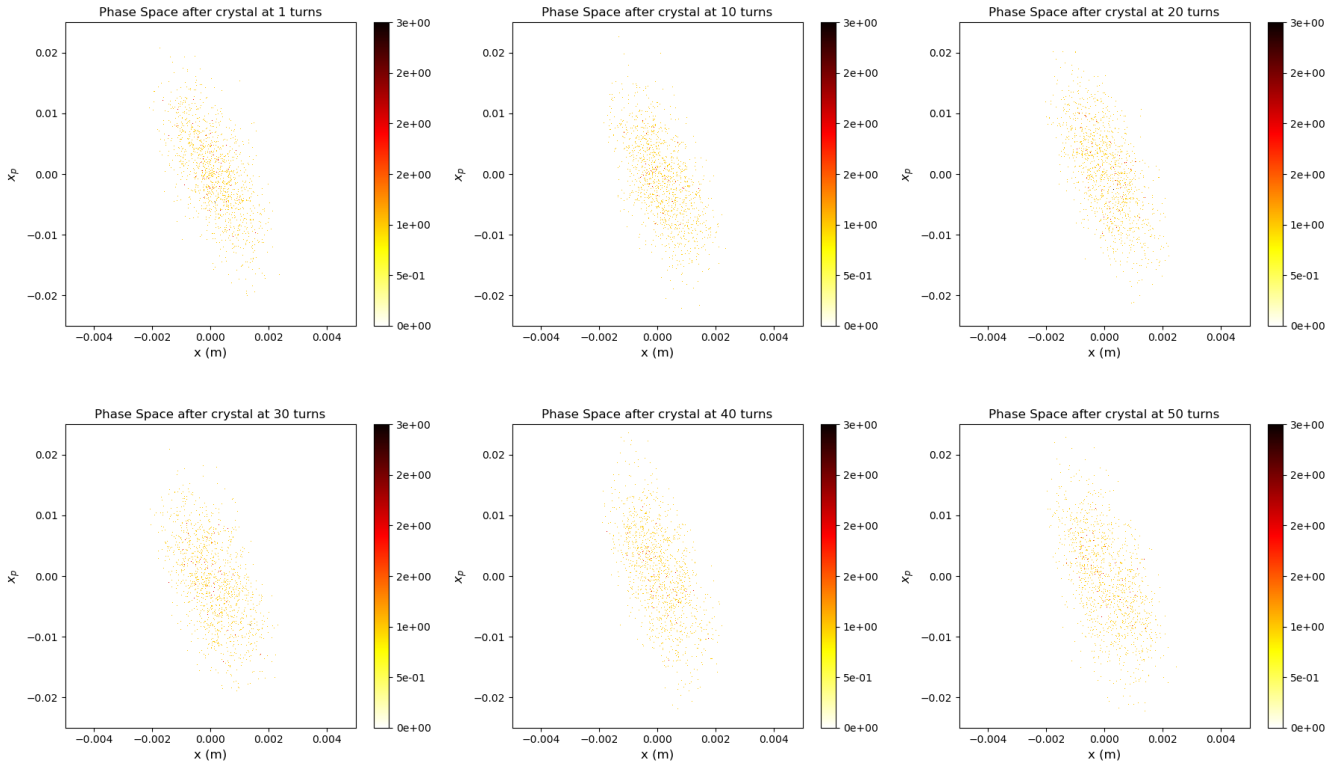

FIG. 11: The phase diagram after the crystal collimator at nth turns. The corresponding turn number can be read from the title.